Journal of Thermal Analysis and Calorimetry, Vol. 61 (2000) 503–512

THE SPECIFIC HEAT OF TETRAMETHYL-AMMONIUM SALTS

I. Ruiz-Larrea[1], *A. Fraile-Rodríguez*[2], *A. Arnáiz*[3] *and A. López-Echarri*[2]

[1]Departamento de Física Aplicada II, Facultad de Ciencias, Universidad del País Vasco
[2]Departamento de Física de la Materia Condensada, Facultad de Ciencias, Universidad del País Vasco
[3]Departamento de Química Inorgánica, Facultad de Ciencias, Universidad del País Vasco Apdo. 644 48080 Bilbao, Spain

Abstract

New measurements of the $(N(CH_3)_4)_2MnBr_4$ specific heat by adiabatic calorimetry around the ferro-paraelastic phase transition shown by the crystal around 276 K are compared with previous calorimetric studies on similar tetramethylammonium bromide compounds. The thermodynamic behaviour of the tribromides and tetrabromides derivatives together with the influence on the phase transition parameters of the cation and halogen molecular substitutions are examined. The thermal relaxation experiments permit to study the behaviour of the crystals thermal conduction as a function of the temperature. Finally, the Landau theory for second order phase transitions is used to describe the thermodynamic behaviour of some of these crystals.

Keywords: adiabatic calorimetry, specific heat, tetramethylammonium salts

Introduction

Crystals with tetramethylammonium groups with the common chemical formula $(N(CH_3)_4)MX_3$ and $(N(CH_3)_4)_2MX_4$ where *M* is a divalent metal such as Mn, Zn, Cd and Hg, and *X* is a halogen, have been widely studied in the last years [1–3, and references therein]. Many of these compounds exhibit successive structural phase transitions which are associated with the reorientational dynamics of the tetramethylammonium groups, $N(CH_3)_4$ (hereafter TMA) as a common feature. Interesting solid phase physical properties such as ferroelectricity, ferroelasticity and even incommensurate crystal structures are commonly found. In some cases, quasi one dimensional magnetic properties are also present at low temperatures. Different calorimetric techniques, including adiabatic calorimetry, have been found very useful to study the wide variety of phase transitions shown by these crystals. The values obtained for the phase transition thermodynamic functions account for the progressive disorder of the TMA groups when the temperature is increased. In some cases [3, and references therein], good fittings of the experimental data to phenomenological models for second order phase transitions are established. One important requirement for this purpose is an accurate separation between the phase transition contribution to the spe-

1418–2874/2000/ $ 5.00
Akadémiai Kiadó, Budapest

cific heat and the normal lattice contribution (the so-called 'baseline'). The combination of the calorimetric data with the lattice vibrational modes, mainly obtained from Raman and IR spectroscopy, together with the specific heat of isomorphous crystals, allow to determine the various contributions to the specific heat, including those of the TMA group. These procedures also permit an estimation of the anharmonic crystal behaviour as a function of the temperature. Interesting solid state physical quantities such as the Gruneisen parameter and the isothermal compressibility, intrinsically difficult to measure by other experimental methods, are easily calculated. Finally, unified pressure-temperature phase diagrams for both series of compounds have been built up in the last years [1, 4–6], and the influence of pressure compared with atom substitutions has also been established [7, 8].

In this work we present new thermodynamic results on $(TMA)_2MnBr_4$ which are also compared with some other bromide derivatives of the tetramethylammonium crystals. Together with the exhaustive investigations carried out with the chloride derivatives of the bistetramethylammonium tetrahalogenmetallates [1], numerous reported works on the bromide compounds of this family are found in the literature. Contrary to the complex phase transition sequences exhibited by the chloride crystals Zn, Co, Mn and Cd tetrabromates only undergo a second order phase transition below room temperature (at 287.8, 287.6, 276.7 and 272.0 K respectively) [9–17].

Up to now, the bistetramethylammonium tetrabromomanganate $(TMA)_2MnBr_4$ has been studied by means of X-ray diffraction [18–21], dielectric measurements under hydrostatic pressure [18, 22], luminescence properties [23] and EPR [24]. This compound presents an orthorhombic structure at room temperature with space group Pnma (Phase I), with the following values for the cell constants: a=12.750(3) Å, b=16.182(3) Å and c=9.301(1) Å, with Z=4 [18, 19]. The structural second order phase transition appears at about 276.5 K and, as observed in other members of this family, is associated with the ordering processes of the TMA groups, together with the common distortion of the organic and inorganic tetrahedra (space group P $2_1/a$).

Experimental

Single crystals of $(TMA)_2MnBr_4$ were grown in an oil bath at 393 K by slow evaporation of acidified aqueous solutions (48% HBr), containing stoichiometric amounts of tetramethylammonium bromide and anhydrous manganese bromide. High purity commercial chemicals were used. Care was taken to avoid crystallization of the chemically related $TMAMnBr_3$ compound. Grown crystals were prismatic and green coloured. After two re-crystallizations, their chemical composition was confirmed by atomic spectroscopy and X-ray diffraction at room temperature. The assignment of the reflections observed was in good agreement with previous results for the cell parameters.

Preliminary DSC measurements on a small sample of $(TMA)_2MnBr_4$ from 130 to 320 K, with varying heating rates from 1 to 10 K min^{-1} were performed. A powdered sample of $(TMA)_2MnBr_4$ was used for the specific heat measurements by adiabatic calorimetry from 60 to 340 K. The adiabatic system and the automatic equip-

ment have been previously described, as well as the various experimental methods available [25, 26]. More recently, improvements both in the data acquisition and in the calorimeter vessel have been done. The vessel was reduced in size as smaller Pt-thermometers (13 mm length and 2 mm in diameter) are now available. The recalibration of the calorimeter by means of a synthetic saphire sample provided by NBS shows an accuracy better than 0.1% in C_p from 10 to 370 K.

Results and discussion

DSC measurements showed the expected phase transition around 276 K. The results did not show traces of any observable thermal hystheresis, in agreement with the second order character assigned to this phase transition. The experimental specific heat data obtained by adiabatic calorimetry are presented in Fig. 1. Only one phase transition was found between 60 and 340 K. Some points were obtained using the conventional pulse method. The heating periods were fixed at 600 s with temperature increments of 1 K, using the facilities provided by the automatic program. The equilibrium times after each heating period vary from 5 to 12 min and show a noticeable increase at the transition temperature and above it. The thermal equilibrium was considered to be attained when the drift temperature (dT/dt) went down to 10^{-6} K s^{-1}. In addition, various heating curves, with rates varying from 0.2 to 4 K h^{-1}, were performed from 250 to 300 K, in order to obtain a better definition of the specific heat curve around the phase transition. Some of these points are also included in Fig. 1. As shown in this plot, the specific heat reaches its maximum at 276.47 K and this value is assigned to the phase transition temperature. The shape of the specific heat curve together with the lack of any observable thermal hystheresis cited above, confirms again the second order character of this phase transition.

In order to obtain the specific heat associated to the phase transition (ΔC_p) and the corresponding thermodynamic functions, different procedures depending on the available experimental information can be used. In the case of the isomorphous $(TMA)_2ZnBr_4$ crystal, the harmonic and anharmonic contributions to C_p were deter-

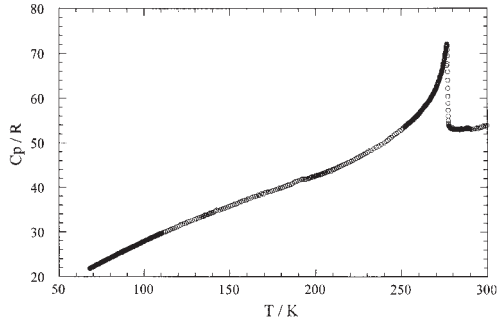

Fig. 1 The specific heat of $(TMA)_2MnBr_4$ from 60 to 300 K obtained by adiabatic calorimetry. Dots represent the experimental points. Only some of them have been plotted for clarity. Both pulse and DSC techniques have been used

mined from group theory, by using spectroscopic, elastic, and expansivity data [27] but up to now this information is not yet available for $(TMA)_2MnBr_4$. However, the experimental specific heat of both crystals shows similar values, exception made of the temperature range where the corresponding phase transitions take place. These results can be seen in Fig. 2 and permit the use of a similar baseline, associated to the lattice specific heat, in order to separate the phase transition contribution. Only a small correction of the Zn baseline, by making use of a corresponding-states law, has been made to better fit the experimental results of the manganese crystal. For this purpose, a re-scaling of the temperature: T'=1.03 T, was done. The subtraction of these baselines from the experimental C_p leads to the evaluation of the specific heat of the phase transition and, by numerical integration, the values for the enthalpy, entropy and free energy thermodynamic functions are also determined.

In the same figure, the specific heat of two tribromide crystals: $TMAMnBr_3$ and $TMACdBr_3$, are also plotted for comparison. The tribromide curves are also similar and permitted us to use the same treatment in order to obtain the phase transition contributions [3, 28]. As in the tetrabromide crystals, they also present one phase transition in this temperature range, but at lower temperatures. However, the characteristics of these phase transitions are quite different. Both are of first order character, with extremely high specific heat peaks (up to 1500 R in $TMACdBr_3$), and involve different symmetry changes: from the common hexagonal room temperature phase ($P6_3/m$) to the monoclinic and ferroelastic low temperature ($P2_1/b$) phase for the manganese compound and to the hexagonal and ferroelectric ($P6_1$) in the case of the cadmium crystal. In addition, another second order phase transition (probably from the hexagonal $P6_3/mmc$ to the hexagonal $P6_3/m$, not shown in the figure and which will not be discussed here), is present in both crystals around 390 K [29].

From previous works about related compounds [30], one should expect that the difference between the lattice contribution (baselines) of both families approximates to the specific heat of the tetramethylammonium bromide compound: (TMA)Br [31]. However, the baselines difference at 300 K is considerably higher (about 25 R) than

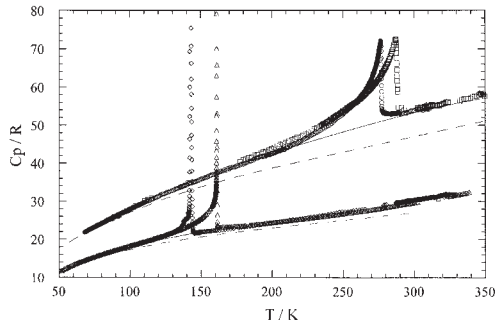

Fig. 2 The specific heat of the tetramethylammonium bromide crystals. $(TMA)_2MnBr_4$[o], $(TMA)_2ZnBr_4$[ ], (TMA)$MnBr_3$[◊] and (TMA)$CdBr_3$[Δ]. The continuous curves are the baselines assigned to the normal lattice contribution. Both dashed lines are the harmonic specific heats, calculated from the frequencies of the vibrational spectrum

the experimental C_p value of (TMA)Br (19.54 R). On the other hand, the difference between the specific heats at constant volume (20.05 R), agrees quite well with this last value. This is a consequence of the very high anharmonic contribution (C_p–C_v) observed in the tetrabromides (up to 14% of C_p), when compared with the tribromide crystals (10%).

Table 1 The specific heat of the tetramethylammonium bromide salts around the phase transition temperatures. $C_p(1)$: $(TMA)_2MnBr_4$, $C_p(2)$: $(TMA)_2ZnBr_4$, $C_p(3)$: $(TMA)MnBr_3$ and $C_p(4)$: $(TMA)CdBr_3$

T/K	$C_p(1)$/R	$C_p(2)$/R	$C_p(3)$/R	$C_p(4)$/R	T/K	$C_p(1)$/R	$C_p(2)$/R	$C_p(3)$/R	$C_p(4)$/R
75	23.22	–	15.22	15.34	210	44.06	45.51	24.84	24.80
80	24.15	–	15.83	15.98	215	44.88	46.29	25.11	25.03
85	25.12	–	16.43	16.59	220	45.77	46.95	25.34	25.27
90	26.07	25.88	16.98	17.17	225	46.80	47.90	25.66	25.49
95	26.96	26.88	17.53	17.74	230	47.85	49.00	25.96	25.73
100	27.89	27.91	18.05	18.29	235	48.93	49.93	26.24	25.96
105	28.78	28.95	18.58	18.84	240	50.06	51.07	26.55	26.21
110	29.69	29.98	19.13	19.40	245	51.60	52.41	26.92	26.45
115	30.44	30.77	19.68	19.96	250	53.01	53.70	27.24	26.73
120	31.26	31.56	20.27	20.54	255	54.58	55.02	27.34	27.02
125	32.14	32.34	20.97	21.14	260	56.45	56.28	27.65	27.24
130	32.86	33.13	21.76	21.79	265	58.84	57.91	27.92	27.45
135	33.64	33.91	22.82	22.49	270	62.04	59.79	28.70	27.73
140	34.43	34.69	25.35	23.29	275	68.47	62.03	29.24	28.01
145	35.06	35.46	21.69	24.21	280	53.11	65.08	29.07	28.38
150	35.81	36.22	21.83	25.42	285	53.03	69.71	29.44	28.66
155	36.56	36.99	22.13	27.26	290	53.09	54.60	29.61	29.00
160	37.20	37.75	22.35	31.63	295	53.42	54.09	30.08	29.30
165	37.99	38.51	22.49	23.19	300	53.93	54.43	30.28	29.61
170	38.59	39.28	22.73	23.28	305	54.09	54.64	30.59	29.96
175	39.25	40.04	22.98	23.42	310	–	55.30	30.85	30.28
180	39.85	40.87	23.22	23.56	315	–	55.16	31.06	30.60
185	40.62	41.58	23.47	23.72	320	–	55.63	31.57	30.91
190	41.52	42.31	23.74	23.93	325	–	56.07	31.77	31.27
195	41.92	43.06	23.99	24.14	330	–	56.30	–	31.67
200	42.54	43.88	24.25	24.35	335	–	56.84	–	32.01
205	43.21	44.77	24.51	24.58	340	–	57.14	–	–

In Table 1 we report the specific heat values at selected temperatures for the four bromide compounds around the phase transition temperatures. After subtracting the corresponding baselines, the behaviour of the phase transition enthalpy and entropy are obtained by numerical integration of the specific heat excess. As we shall see later, the entropy values are related with the order parameter behaviour near the phase transition temperature in the frame of the Landau model. The phase transition temperatures, as well as the total thermodynamic function values for these compounds can be seen in Table 2. The high entropy values shown by the four compounds accounts for the expected disorder attained by the tetramethylammnium groups in the high temperature phase. This is the only common characteristic found in these phase transitons, though the detailed disorder features are far from being established. The high temperature factors observed by X-ray diffraction at room temperature, together with the presence of different domains in the low temperature phases, do not allow a precise determination of the tetramethylammonium positions in many cases. In fact, the number of possible reorientations of the organic groups and the theoretical models used for the description of the physical mechanisms of these phase transitions are still under discussion. In the case of the tribromide crystals, Frenkel models for two, three, or six-potential wells have been examined [3, 32–34] but some doubts remain about the number of different configurations which are accessible to the TMA groups. Moreover, the entropy results presented here do not permit to choose among the different alternatives and claim for a wider experimental work. For example, the phase transition entropy values for the bromide compounds are found to be higher than those for the chloride ones (0.99 R for $TMACdCl_3$ and 1.02 R for $TMAMnCl_3$, which suggested three independent orientations for the TMA groups) and the same result stands for the tetrahalogen crystals [8]. This is related to the higher atomic packing of the crystal unit cell when the chlorine-bromine substitution takes place. Moreover, the phase transition significantly alters this atomic packing. As regards the tribromide crystals, the axial and rigid structure shown by the inorganic octahedra chains along the hexagonal axis, explains the higher thermal expansion in the perpendicular plane. It implies an increase of near 1% for the cell dimensions *a* and *b* in the hexagonal phase when going from the low temperature phase to room temperature. The corresponding separation of the inorganic chains favours the reorientational disorder of the tetramethylammonium groups. Finally, as it can be seeen in this table, the phase transition entropy is higher when the transition temperature increases. All these facts, together with the pressure-temperature phase diagrams [4, 5], suggest that the available cell volume for the TMA groups, which can be altered by cation substitution or by hydrostatic pressure as well, plays a relevant role in the actual values of the phase transition parameters (temperature, total entropy, etc.).

As cited above, a noticeable increase of the thermal relaxation times are found in the high temperature phase of the bromide salts. This should be a direct consequence of the structural disorder observed in these phases, which affects the lattice phonon scattering and the corresponding thermal conduction parameters [35]. Relative values of the sample thermal diffusivity of the crystal as a function of temperature can be obtained when the conventional pulse method is used in adiabatic calorimetry. The au-

tomatic data acquisition permits to measure the thermal relaxation of the sample+calorimetric vessel after each heating period. The temperature *vs.* time curves obtained after each heating pulse are found to fit quite well an empirical relaxation law of the form [26]: $T=T_{eq}+Ae^{-t/\tau_1}+Be^{-t/\tau_2}$ where T_{eq} is the final equilibrium temperature, A and B are constants with no physical relevance ($A+B$ is the initial temperature), and τ_1 and τ_2 are two relaxation times. The use of the two exponential terms is required by the presence of two different physical systems: one is the sample itself and the other the copper vessel and addenda, usually with very much lower relaxation times. Mean least squares fits to this law lead to very low standard deviation values, lying between 0.0005 and 0.003 in the 60–300 K temperature range. As an example, taken from the measurements performed on $TMAMnBr_3$, one of these fits which allows to determine both τ_1 and τ_2 is presented in Fig. 3. As expected, these quantities vary with the temperature range, so they depend on the final equilibrium temperature (T_{eq}) and represent the relaxation of the system at this temperature. In Fig. 4 we have plotted all these results, including τ_1 and τ_2 as a function of T_{eq}. The lower relaxation time τ_1, which slightly increases with temperature, must be associated with the vessel system, due to the high thermal conductivity of its metallic components, whereas τ_2 is associated to the sample. This fact is firmly supported by the absence of a significant anomaly of τ_1 around the phase transition temperature. However, at this temperature the values of τ_2 clearly show the expected increase in proximity of a phase transition, where the thermal conduction of dielectric materials is very poor. Above this temperature, the sample relaxation time τ_2 is in this case about 40% higher in the hexagonal high temperature phase than in the monoclinic one.

Table 2 The integrated phase transition thermodynamic functions of the tetramethylammonium bromide salts

Compound	Phases	T_c/K	ΔH/R K	ΔS/R
$[TMA]_2ZnBr_4$	Pnma→$P2_1/a$	287.19	490±30	1.95±0.1
$[TMA]_2MnBr_4$	Pnma→$P2_1/a$	276.47	374±30	1.43±0.1
$[TMA]CdBr_3$	$P6_3/m$→$P6_1$	161.30	316±30	2.18±0.1
$[TMA]MnBr_3$	$P6_3/m$→$P2_1/b$	142.55	218±10	1.58±0.1

The relaxation time values obtained by this method are directly dependent on the experimental conditions. The amount of sample, the powder size distribution, or the helium pressure inside the vessel, as well as many other variables, affect the values obtained for τ_1 and τ_2 , so absolute results can not be established. However, as these parameters can be considered to be constant in our experiments, they provide enough information about the relative behaviour of the thermal diffusivity of the crystal *vs.* temperature. It should be noted that the relaxation curves are measured after heating periods of identical characteristics: same heating times and same temperature increments, always under the control of the adiabatic shield. This explains the good agreement of the four different runs presented in Fig. 4. However, the inadequacy of the experimental set-up for this kind of measurements (the asymmetries of the vessel sys-

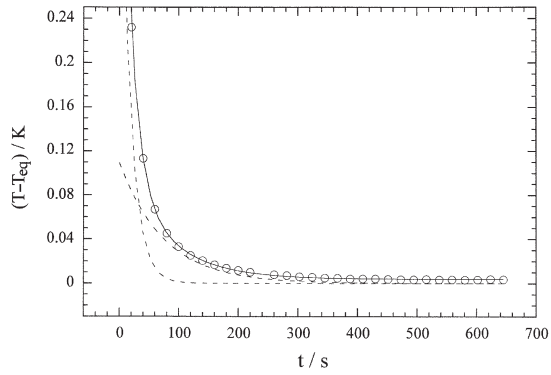

Fig. 3 An example of a thermal relaxation curve for (TMA)$MnBr_3$. Points represent the measured temperature *vs.* time after a heating pulse (1°C in 600 s). The final equilibrium temperature was in this case T_{eq}=81.874 K. Points are fitted to an exponential law $T-T_{eq}=Ae^{-t/\tau_1}+Be^{-t/\tau_2}$ (continuous curve). The dashed curves represent the two exponential terms associated to the fast thermal relaxation of the vessel system and to the lower one of the sample. The standard deviation is 0.00048. The fitted parameter values are: A=0.4733, B=0.1093, τ_1=16.97 s and τ_2=74.86 s

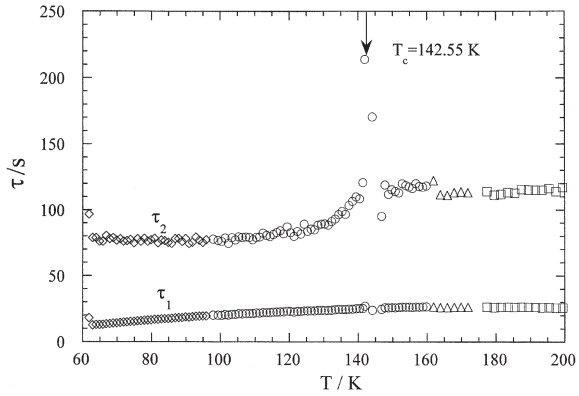

Fig. 4 The thermal relaxation times τ_1 and τ_2 of (TMA)$MnBr_3$ *vs.* temperature. Four different runs are plotted. τ_1 is insensitive to the phase transition at about 143 K. However, τ_2 shows a noticeable jump at this temperature

tem, the unknown thermal gradients inside the sample, etc.) excludes further calculations which could lead to quantitative and accurate values for the thermal conduction parameters of the crystal.

Up to now some attempts to describe the phase transition in $TMACdBr_3$ and isomorphous crystals by phenomenological approaches have been made [3], but new doubts about the symmetry assignments [36] prevent conclusive results from giving. Similarly, the thermodynamic properties of the phase transition exhibited by

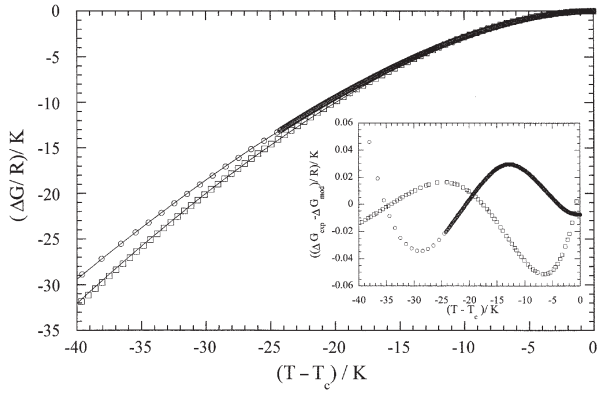

Fig. 5 The phase transition experimental free energy of $(TMA)_2ZnBr_4$ [ ] and $(TMA)_2MnBr_4$ [o] fitted to the Landau model (continuous lines). The insert shows the deviations between the experimental values and the theoretical curves

$(TMA)_2MnBr_4$ and $(TMA)_2ZnBr_4$ can be easily described within the frame of the Landau theory for second order phase transitions [27]. Using the same model for both compounds, the experimental free energy can be adequately fitted to the simple Landau expansion as a function of the order parameter (Q):

$$F=\frac{1}{2}\alpha(T-T_c)Q^2+\frac{1}{4}\beta Q^4+\frac{1}{6}\gamma Q^6+\frac{1}{8}\delta Q^8 \quad (1)$$

The behaviour of Q near the phase transition temperature can be estimated from the entropy values using the relation:

$$S=-\frac{\partial F}{\partial T}=-\frac{1}{2}aQ^2$$

The results of these fittings are shown in Fig. 5 for comparison, with the coefficient values in Table 3. A good agreement down to 40 K below the transition temperature is obtained. Further developments of this model in order to describe the ferrielastic properties observed in these crystals are now in progress.

Table 3 Phenomenological coefficients of Eq. (1) for the phase transition of $(TMA)_2MnBr_4$ and $(TMA)_2ZnBr_4$. Units are choosen so that F is in R units

	α	β	γ	δ
$(TMA)_2ZnBr_4$	1	7.307	1.023	0.708
$(TMA)_2MnBr_4$	1	6.558	2.320	0.910

* * *

This work was supported by the Universidad del País Vasco under projects UPV 060.310-EB069/96 and UPV 063.310-G16/98.

References

1 K. Gesi, Ferroelectrics, 66 (1986) 269.
2 M. N. Braud, M. Couzi and N. B. Chanh, J. Phys.: Condens. Matter, 2 (1990) 8243.
3 G. Aguirre-Zamalloa, J. M. Igartua, M. Couzi and A. López-Echarri, J.Phys. I France, 4 (1994) 1237.
4 H. Shimizu, A. Oguri, N. Abe, N. Yasuda, S. Fujimoto, S. Sawada, Y. Shiroishi and M. Takashige, Solid State Commun., 29 (1979) 125.
5 P. S. Peercy, D. Morosin and G. A. Samara, Phys. Rev. B, 7 (1973) 3378.
6 M. Couzi and Y. Mlik, J. Raman Spectrosc., 17 (1986) 117.
7 R. Perret and G. Godefroy, Ferroelectrics, 73 (1987) 87.
8 A. López-Echarri, I. Ruíz-Larrea and M. J. Tello, Phys. Stat. Sol, 154 (1989) 143.
9 K. Gesi and K. Ozawa, J. Phys. Soc. Japan, 51 (1982) 2205.
10 G. Madariaga, F. J. Zúñiga and W. A. Paciorek, Acta Cryst., B46 (1990) 620.
11 K. Aizu, J. Phys. Soc. Japan, 27 (1969) 387.
12 A. Sawada, J. Phys. Soc. Japan, 60 (1991) 3593.
13 A. Sawada, Ferroelectrics, 191 (1997) 349.
14 T. Asahi, K. Hasebe and K. Gesi, J. Phys. Soc. Japan, 61 (1992) 1590.
15 S. Harada, M. Iwata and Y. Ishibashi, J. Phys. Soc. Japan, 61 (1992) 3436.
16 A. Sawada, H. Matsumoto and K. Tanaka, Ferroelectrics, 140 (1993) 245.
17 R. Valiente, M. C. Marco de Lucas and F. Rodríguez, J. Phys.: Condens. Matter, 7 (1995) 3881.
18 K. Gesi, J. Phys. Soc. Japan, 52 (1983) 2931.
19 K. Hasebe and T. Asahi, Acta Cryst., C45 (1989) 841.
20 K. Hasebe, T. Asahi and K. Gesi, Acta Cryst., C46 (1990) 759.
21 T. Asahi and K. Hasebe, J. Phys. Soc. Japan, 63 (1994) 2827.
22 K. Tanaka and A. Sawada, Ferroelectrics, 159 (1994) 221.
23 M. C. Marco de Lucas and F. Rodríguez, J. Phys.: Condens. Matter, 5 (1993) 2625.
24 W. Zapart, J. Solecki, M. B. Zapart, A. Sawada and K. Tanaka, J. Korean Phys. Soc., 32 (1998) S697.
25 A. López-Echarri and M. J. Tello, J. Phys. D, 14 (1981) 71.
26 J. Zubillaga, A. López-Echarri and M. J. Tello, Thermochim. Acta, 92 (1981) 283.
27 J. M. Igartua, I. Ruiz-Larrea, M. Couzi, A. López-Echarri and T. Breczewski, Phys. Stat. Sol. (b) 168 (1991) 67.
28 I. Ruiz-Larrea, J. Díaz-Hernández, A. Fraile-Rodríguez, A. Arnaiz and A. López-Echarri, J. Phys.: Condens. Matter, in press.
29 P. Vanek, M. Havranova, M. Smutny and B. Brezina, Ferroelectrics, 109 (1990) 51.
30 A. López-Echarri, I. Ruiz-Larrea and M. J. Tello, J. Phys.: Condens. Matter, 2 (1990) 513.
31 S. S. Chang and E. F. Westrum, J. Chem. Phys., 36 (1961) 2420.
32 J. Díaz-Hernández, G. Aguirre-Zamalloa, A. López-Echarri, T. Breczewsky and M. J. Tello, J. Phys.: Condens. Matter, 9 (1997) 3399.
33 M. Jewes, Acta Cryst., B38 (1982) 1418.
34 G. Aguirre-Zamalloa, G. Madariaga, M. Couzi and T. Breczewski, Acta Cryst., B49 (1993) 691.
35 J. E. Parrot and A.D. Stuckes, Thermal Conductivity of Solids, Pion Limited, London 1975.
36 I. Peral, G. Madariaga, A. Pérez-Etxebarria and T. Breczewski, Acta Cryst. B (in press).